

## Dimerisation of *N*-acetyl-L-tyrosine ethyl ester and A $\beta$ peptides via formation of dityrosine

FEDA E. ALI<sup>1,2</sup>, ANDREW LEUNG<sup>1</sup>, ROBERT A. CHERNY<sup>2</sup>, CHRISTINE MAVROS<sup>2</sup>, KEVIN J. BARNHAM<sup>2</sup>, FRANCES SEPAROVIC<sup>1</sup>, & COLIN J. BARROW<sup>1</sup>

<sup>1</sup>*School of Chemistry, University of Melbourne, Melbourne, VIC 3010, Australia, and* <sup>2</sup>*Department of Pathology and The Mental Health Research Institute of Victoria, University of Melbourne, Melbourne, VIC 3010, Australia*

Accepted by Professor M. Davies

(Received 30 March 2005; in revised form 2 August 2005)

### Abstract

Alzheimer's disease (AD) is characterised by the formation of amyloid deposits composed primarily of the amyloid  $\beta$ -peptide (A $\beta$ ). This peptide has been shown to bind redox active metals ions such as copper and iron, leading to the production of reactive oxygen species (ROS) and formation of hydrogen peroxide (H<sub>2</sub>O<sub>2</sub>). The generation of H<sub>2</sub>O<sub>2</sub> has been linked with A $\beta$  neurotoxicity and neurodegeneration in AD. Because of the relative stability of a tyrosyl radical, the tyrosine residue (Tyr-10) is believed to be critical to the neurotoxicity of A $\beta$ . This residue has also been shown to be important to A $\beta$  aggregation and amyloid formation. It is possible that the formation of an A $\beta$  tyrosyl radical leads to increased aggregation via the formation of dityrosine as an early aggregation step, which is supported by the identification of dityrosine in amyloid plaque. The role of dityrosine formation in A $\beta$  aggregation and neurotoxicity is as yet undetermined, partly because there are no facile methods for the synthesis of A $\beta$  dimers containing dityrosine. Here we report the use of horseradish peroxidase and H<sub>2</sub>O<sub>2</sub> to dimerise *N*-acetyl-L-tyrosine ethyl ester and apply the optimised conditions for dityrosine formation to fully unprotected A $\beta$  peptides. We also report a simple fluorescent plate reader method for monitoring A $\beta$  dimerisation via dityrosine formation.

**Keywords:** *Alzheimer's disease, amyloid  $\beta$  peptide, horseradish peroxidase, metal catalyzed oxidation, oxidative stress, dityrosine*

**Abbreviations:** ATEE, *N*-acetyl tyrosyl ethyl ester; AD, Alzheimer's disease; A $\beta$ , Amyloid  $\beta$  peptide; APP,  $\beta$  amyloid precursor protein; Boc, *t*-Butyloxycarbonyl; DOPA, 3, 4-dihydroxyphenylalanine; ECL, enhanced chemiluminescence; ESI-MS, Electrospray-ionization mass spectrometry; HFIP, hexafluoroisopropanol; MCA, multichannel analysis mode; MCO, Metal catalysed oxidation; NFT, intracellular neurofibrillar tangles; OH, hydroxyl radical; PBS, Phosphate buffered saline; ROS, Reactive oxygen species; RP-HPLC, Reversed phase-high performance liquid chromatography; SDS, sodium dodecyl sulphate; TR, Tyrosyl radical

### Introduction

There is growing support for the involvement of free radicals in A $\beta$  associated neurotoxicity in Alzheimer's disease (AD) [1]. Recent work has identified specific amino acids in the A $\beta$  sequence that are involved in free radical generation, either via an ability to bind metals such as Cu<sup>2+</sup>, or through their ability to stabilise or transfer an electron [2]. For example, the

(His)XXX(Tyr)XX(His) motif in the A $\beta$  peptide sequence (Figure 1) appears to be crucial for oxidative damage to the  $\beta$  amyloid precursor protein (APP) in the initial stages of free-radical-based pathogenesis in AD[3]. The sole tyrosine residue in the A $\beta$  sequence is within this motif (Tyr 10) and is in close proximity to the Cu<sup>2+</sup> binding site containing the histidines residues [3,4]. Tyr 10 has been identified as an

Correspondence: C. J. Barrow, Ocean Nutrition Canada, 101 Research Drive, Dartmouth, NS, B2Y 4T6, Canada. Tel: 1 902 480 3248. Fax: 1 902 480 3248. E-mail: cbarrow@ocean-nutrition.com

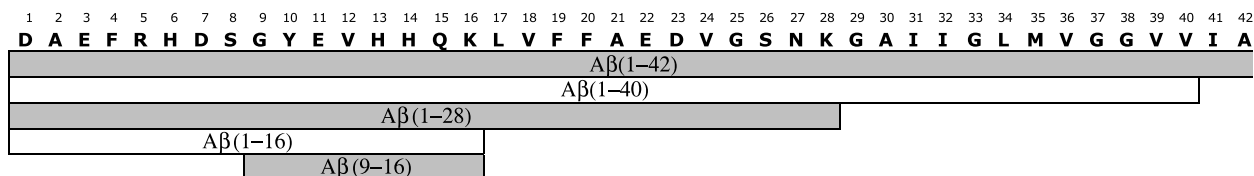


Figure 1. Amino acid sequence of A $\beta$  peptides. Both tyrosine-10 and methionine-35 play a role in ROS formation and histidines 6, 13 and 14 are the metal binding sites.

important amino acid in the aggregation and amyloidogenicity of A $\beta$  [5,6].

The importance of Tyr 10 in A $\beta$  amyloid formation and associated neurotoxicity may be partly due to the ability of Tyr 10 to form a stable radical during metal catalysed oxidation (MCO), since the proximity of Tyr 10 to the neighbouring histidines residues allows a redox active metal ion such as Cu<sup>2+</sup> to extract one electron to form a tyrosine radical [7–9]. The most stable structures resulting from tyrosine radical coupling include formation of protein-bound dityrosine (C<sub>ortho</sub>–C<sub>ortho</sub> coupling) and isodityrosine (C<sub>ortho</sub>–O coupling) [10,11]. The principles of this dimerisation are shown in Scheme 1.

Dityrosine bridges in peptides and proteins are formed by many ubiquitous processes in biological systems leading to protein degradation and cellular damage [12], including ultraviolet irradiation of calmodulin [13–15], peroxidation of membrane lipids [16], the inflammatory response by the action of some peroxidase enzyme systems like myeloperoxidase (MPO) and Hydrogen Peroxide (H<sub>2</sub>O<sub>2</sub>) [17–25] or by polymorphonuclear leukocytes [26], and by the action of an enzymatic alternative to peroxidase inside the mitochondrion [27,28]. Dityrosine has also been chemically identified in tissues associated with some diseases including AD [29,30]. There are few studies that attempt to relate the oxidation of tyrosine to senile plaque formation in AD [9,31–32], although there is some data indicating that A $\beta$  dityrosine formation occurs during amyloid formation and may be important in A $\beta$  associated neurotoxicity and associated neurodegeneration [29,33]. The formation of A $\beta$

dimers through the phenolic coupling of tyrosine could be an early event critical to fibril formation and A $\beta$  deposits in AD [31].

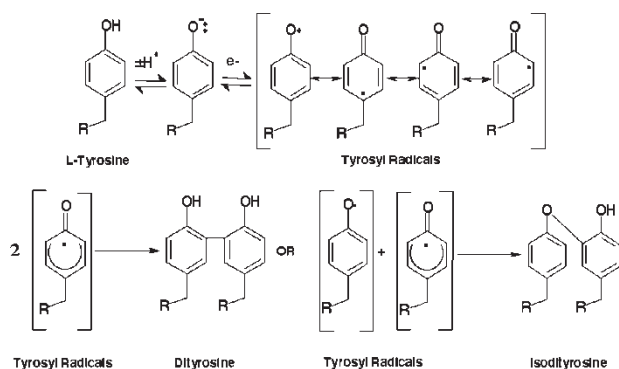
There have been limited studies of dityrosine, in particular, dityrosine-containing dimeric peptides, partly because of the difficulty in synthesising these systems. Synthesis and study of dityrosine-containing A $\beta$  dimeric peptides could lead to a better understanding of the importance of A $\beta$  oxidative modification and dimerisation in amyloid formation and AD associated neurodegeneration. In the current study, we have modified a method for dimerising peptide-bound tyrosine residues in reasonable yield using chemically unprotected peptides [6]. The method uses horseradish peroxidase in the presence of H<sub>2</sub>O<sub>2</sub> and is derived from a method applied to forming dityrosine in unprotected cyclic tetrapeptides [34]. We initially applied this method to the dimerisation of the model compound *N*-acetyl-L-tyrosine ethyl ester (ATEE) and subsequently to A $\beta$ (9–16), an A $\beta$  model peptide containing Tyr-10 plus two of the oxidatively sensitive histidine residues. After obtaining high yields of dimeric peptides for A $\beta$ (9–16) we applied the same conditions to the dimerisation of A $\beta$ (1–28) and A $\beta$ (1–40) and used fluorescent and antibody detection methods to monitor the formation of dimers and higher oligomers.

## Experimental procedures

### Chemicals and materials

BDH Chemicals (Poole, England) was the source of H<sub>2</sub>O<sub>2</sub> (30%), sodium phosphate, ethyl acetate, ammonium carbonate and other buffers and salts (Analar grade). BDH (Poole, England) and Merck (Darmstadt, Germany) supplied the organic solvents (HiPerSolv for HPLC). ATEE, 2-mercaptoethanol, Chelex 100 and DEAES Sephadex were purchased from Sigma Chemical Co. (St Louis, USA). All other reagents were of the highest grade. HRP was compared to commercially available HRP type VI-A (purchased from Sigma Chemical Co.) and resulted in higher dityrosine formation.

Electrophoretic molecular weight markers and reagents for enhanced chemiluminescence (ECL) were purchased from Amersham Pharmacia Biotech (Sydney, Australia). Electrophoretic reagents and



Scheme 1.

Trans-Blot nitrocellulose membrane were obtained from BioRad Laboratories (Sydney, Australia).

A $\beta$ (9–16), A $\beta$ (1–28) and A $\beta$ (1–40) were synthesized utilizing manual solid-phase chemistry as described by He and Barrow [35] using *N*-tert-butylloxycarbonyl (Boc) amino acid chemistry and PAM resin. After hydrogen fluoride cleavage of the peptides from the resin the crude peptide was purified by HPLC. Peptide purity and identity were confirmed by HPLC, ESI-MS and amino acid analysis.

### Instrumentation

RP-HPLC was performed using Beckman System Gold model 126-pump and Beckman System Gold Diode array detector Module 168 (Fullerton, USA) and recorded using Nouveau Gold software package. UV–Vis and fluorescence spectra were acquired in a 10 or 4 mm quartz cuvette using a Shimadzu UV-2401PC UV–Vis recording spectrophotometer (Kyoto, Japan) and a Varian Cary 50 Bio UV–Vis spectrophotometer (Melbourne, Australia), and a Varian Cary Eclipse fluorescence spectrophotometer (Melbourne, Australia). Some samples were analysed using fMax Fluorescence Microplate Reader with incubator and SOFT maxPRO software (Sunnyvale, USA). Fluorescence plate reader measurements were carried at 25°C using filters of ( $\lambda_{\text{ex}}$ 355 nm/ $\lambda_{\text{em}}$ 460 nm,  $\lambda_{\text{ex}}$ 485 nm/ $\lambda_{\text{em}}$ 538 nm,  $\lambda_{\text{ex}}$ 544 nm/ $\lambda_{\text{em}}$ 590 nm and  $\lambda_{\text{ex}}$ 584 nm/ $\lambda_{\text{em}}$ 612 nm). ESI-MS were acquired using a Micromass Quattro II triple quadrupole instrument (Manchester, UK) in Positive Ion Mode, connected to a Hewlett Packard (HP1100) LC system (Palo Alto, USA). Samples were dissolved in 1% formic acid and buffer solutions of either 0.1% formic acid or ammonium formate in MilliQ water: acetonitrile (50:50), were fed at 40  $\mu$ l/min to the MS probe.  $^1\text{H}$  and  $^{13}\text{C}$  NMR spectra were recorded using a Varian (Palo Alto, USA) Unity plus spectrometer operating at 400 MHz for protons. Infrared spectra were acquired on a Bio-Rad FTS-165 Fourier-transform infrared spectrophotometer (Hercules, USA).

### Dimerisation of *N*-acetyl-L-tyrosine ethyl ester (ATEE)

ATEE (0.2045 g, 0.8 mmole) was dissolved in borate buffer (100 ml, 0.1 M, pH 9.1). The sealed reaction vessel was immersed in a 37°C water bath under an argon or nitrogen atmosphere. Then 250  $\mu$ l of freshly prepared HRP solution (4 mg/1 ml) was added while stirring. Three aliquots of 100  $\mu$ l of the solution were transferred immediately by a syringe to a 1 ml vial and 2  $\mu$ l of 2-mercaptoethanol was added to stop the reaction and the solution freeze-dried. These aliquots were used as the zero time reaction controls. To the remaining reaction mixture was added 85  $\mu$ l of 30% of  $\text{H}_2\text{O}_2$  solution (0.8 mmole). After 2 min, the reaction

was quenched by addition of 2-mercaptoethanol (25  $\mu$ l). Another three aliquots of 100  $\mu$ l were transferred and tested as end reaction samples. All samples were frozen in liquid nitrogen and freeze dried. The product was desalted using flash C18 chromatography, eluting with methanol and water (1:1) and the reaction mixture analysed by RP-HPLC using a Zorbax 300SB column. Peaks were observed corresponding to ATEE, diATEE, isodiATEE and triATEE, eluting in that order (Figure 2). The major product, diATEE, was purified by semi-preparative RP-HPLC. A yield of 45% diATEE was obtained, based on weight of desalted product. Analytical RP-HPLC on the purified diATEE indicated a purity of greater than 99%.

The overall yield of diATEE from tyrosine was 29 ( $\pm 3$ )%. ESI-MS  $m/z$  501 [ $M + H$ ].  $^1\text{H}$  NMR (400 MHz,  $\text{CD}_3\text{OD}$ ): 1.08 (6H, t), 1.81 (6H, s), 2.81 (2H, dd,  $J = 8$  Hz), 2.95 (2H, dd,  $J = 6$  Hz), 4.01 (4H, q), 4.49 (2H, q), 6.73 (2H, d,  $J = 8$  Hz), 6.92 (1H, d,  $J = 2$  Hz), 6.94 (3H, m) (Figure 4(b)).  $^{13}\text{C}$  NMR (125 MHz,  $\text{CD}_3\text{OD}$ ): 15.7, 23.5, 50.2, 56.8, 63.3, 118.5, 128.5, 130.7, 132.3, 135.8, 155.4, 174.4. IR  $\nu_{\text{max}}$  3434, 1736, 1643, 1564  $\text{cm}^{-1}$ .

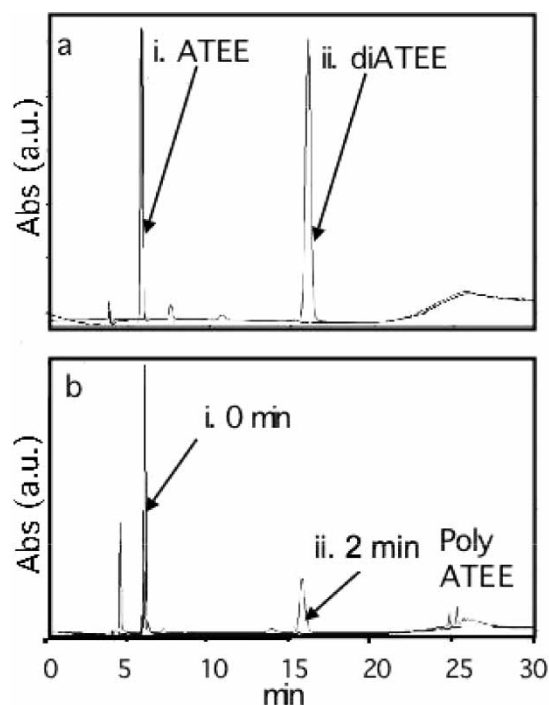


Figure 2. Chromatogram of: (a) ATEE and diATEE subjected to HPLC analysis on a RP C<sub>18</sub> column (Zorbax 300SB, 250  $\times$  4.6 mm, 5  $\mu$ m) using 1 ml/min flow rate, 45% methanol and 0.1% of trifluoroacetic acid in water for 15 min, followed by 5 min linear gradient to 80% methanol fixed for 5 min and then returned back to initial conditions within 5 min using linear gradients (where (i) and (ii) are 1.6 mM ATEE and 0.8 mM diATEE standards, respectively) and (b) the crude reaction mixture of ATEE at (i) the start or 0 min, and (ii) the end after 2 min of reaction.

### Time course monitoring of ATEE dimerisation

A closed vial containing 7.5 mg of ATEE (30  $\mu$ mole) dissolved in 4 ml of either phosphate buffer pH 7.4 or borate buffer pH 9.1 (10 mM) was placed in a water bath at 37°C. While stirring, the vial was purged with nitrogen for 10 min. Then 10  $\mu$ l of freshly prepared HRP solution in MilliQ water (0.3 mg/10  $\mu$ l) was added. A measured quantity of 100  $\mu$ l of the solution was removed from the closed vial using a syringe and transferred to a 1 ml Eppendorf vial. The reaction was stopped by the addition of 1  $\mu$ l of 2-mercaptoethanol, the sample freeze dried and used as the zero time reaction. To the remaining reaction mixture was added 34  $\mu$ l of 3% of H<sub>2</sub>O<sub>2</sub> (30  $\mu$ mole). Hundred microlitres of the reaction mixture was removed at a specific time intervals (2, 4, 6, 10, 60 min and 24 h). After freeze-drying, the samples were analysed by HPLC to monitor the formation of the dimer.

### Dimerisation of A $\beta$ (9–16)

A $\beta$ (9–16) (10 mg, 10  $\mu$ mole) was dissolved in borate buffer (40 ml, 0.1 M, pH 9.1). The sealed reaction vessel with a magnetic stirrer was immersed in a 37°C water bath and purged with nitrogen gas for 10 min. Two hundred microlitres of fresh prepared HRP solution (0.2 mg/200  $\mu$ l) was added while stirring. Hundred microlitre of the solution were transferred immediately to use as the zero time reaction, 2  $\mu$ l of 2-mercaptoethanol added to stop the reaction and then freeze-dried. To the remaining reaction mixture was added 0.15% w/v H<sub>2</sub>O<sub>2</sub> solution freshly prepared from a 30% H<sub>2</sub>O<sub>2</sub> stock solution (114  $\mu$ l, 5  $\mu$ mole). After 15 min, the reaction was stopped by addition of 2-mercaptoethanol (30  $\mu$ l). The reaction product was analysed by RP-HPLC with diA $\beta$ (9–16) being the major product. A $\beta$ (9–16) was purified using semi-preparative RP-HPLC and recovered with an overall yield from starting peptide of 22% yield. ESI-MS confirmed the presence of a dimer and amino acid analysis was consistent with the expected product. ESI-MS  $m/z$  1992.8 ( $[M + H]^+$  expected 1993.2); Amino acid analysis: Gln/Glu 4.8 (4), Gly 1.87 (2), His 3.7 (4), Lys 2.0 (2), Tyr 0.0 (0), Val 2.0 (2).

### Time course monitoring of A $\beta$ (9–16) peptide dimerisation

The same procedure as for the A $\beta$ (9–16) dimerisation reaction was followed on a 1 mg scale. Two hundred and fifty microlitres of aliquots of the reaction solution were taken at times 0, 1, 2, 3, 4, 5, 10, 15, 20, 30, 40, 60 and 80 min and each quenched with 1  $\mu$ l of 2-mercaptoethanol. The remaining solution was left for a further 80 min and quenched with 5  $\mu$ l of 2-mercaptoethanol. All samples were frozen in liquid nitrogen and freeze dried. The samples were analysed for yield of dimer by RP-HPLC.

### UV-visible and fluorescence monitoring of A $\beta$ (9–16) reaction

Samples were dissolved in MilliQ water and 5  $\mu$ l aliquots were injected into 245  $\mu$ l of 0.5 mM borate buffer in a 4 mm quartz cell, and analysed at room temperature using Cary Eclipse UV-Vis and fluorescence spectrophotometers. The absorbance between 180 and 800 nm were measured for UV-Vis spectra. The fluorescence spectra were scanned at different excitation values:  $\lambda_{ex}$ 274 nm/ $\lambda_{em}$  scanned from 280–550 nm and  $\lambda_{ex}$ 325 nm/ $\lambda_{em}$  scanned from 330–640 nm using 5 nm slit width.

### Dimerisation of A $\beta$ (1–40) and A $\beta$ (1–28)

Solutions of A $\beta$ (1–28) and A $\beta$ (1–40) were dimerised as described in Table I. ATEE was used as a control to monitor the formation of dimers. The reaction was started by the addition of 100  $\mu$ l of (30  $\mu$ mole) H<sub>2</sub>O<sub>2</sub>, and all vials were incubated at 37°C for 6 h. The samples were then frozen under liquid nitrogen, freeze dried and analysed using ESI-MS, fluorescence plate reader and Western blot gel (WO2).

### Gel electrophoresis monitoring of A $\beta$ (1–28) and A $\beta$ (1–40) dimerisation reactions

To monitor the dimerisation of A $\beta$ (1–28) and A $\beta$ (1–40), gel electrophoresis-polyacrylamide gel electrophoresis was performed in the presence of SDS (SDS-PAGE). The dried samples were diluted  $\times 10$  (2  $\mu$ l in 20  $\mu$ l) using sample buffer (8 M urea, 8%

Table I. Composition of reaction solutions for dimerisation of A $\beta$ (1–40) and A $\beta$ (1–28).

Reaction Solution	Volume of solutions ( $\mu$ l)				
	Acetate buffer*	HRP†	A $\beta$ (1–28)‡	A $\beta$ (1–40)¶	ATEE§
A $\beta$ (1–28)	750	100	50	–	–
A $\beta$ (1–40)	765	100	–	35	–
ATEE	700	100	–	–	100

\*0.1 M acetate buffer pH 7.4. †0.4 mg/ml of HRP in buffer. ‡0.2 mg/ml of A $\beta$ (1–28) in  $\eta$ -hexafluoroisopropanol (HFIP). ¶0.4 mg/ml of A $\beta$ (1–40) in HFIP. §0.07 mg/ml of ATEE in buffer.

SDS, 30% glycerol, 100 mM tricine, 0.01% phenol red and 10% mercaptoethanol), then gel electrophoresis was run according to the procedure of Cherny et al. [36]. Using the primary monoclonal mouse antibody, WO2 in conjunction with horseradish peroxidase-conjugated rabbit anti-mouse IgG (Dako, Denmark), and visualized using chemiluminescence (ECL, Amersham Pharmacia Biotech) [36]. The epitope for WO2 is residues 5–8 of A $\beta$  [37].

## Results and discussion

### Dimerisation of *N*-acetyl-*L*-tyrosine ethyl ester

ATEE was used as a model for the dimerisation of peptide tyrosine residues to enable easier analysis of reaction products while developing reaction conditions for peptide dimerisation. Chemical reaction conditions were tested initially, including MCO systems such as Cu<sup>2+</sup> plus H<sub>2</sub>O<sub>2</sub> with and without methionine [38]. However, these chemical conditions gave very low reaction yields of dimers and most resulted mainly in recovery of unreacted starting material. The use of the enzyme horseradish peroxidase in the presence of H<sub>2</sub>O<sub>2</sub> under appropriate conditions did lead to the formation of ATEE dimers in relatively good yield. The method was developed based on a method previously employed to produce dimeric cyclic peptides [39]. The reactivity of HRP was previously shown to be optimum at alkaline pH. Alkaline pH has been shown to decrease the aggregation of A $\beta$  peptides and increase their solubility. However, too alkaline, a pH can result in destruction or racemisation of sensitive residues in some peptides. Therefore, we compared the dimerisation of ATEE at neutral pH and slightly basic pH to determine if pH significantly impacted the products formed in addition to the reaction rate. The results of a time course study of ATEE dimerisation at pH 7.4 and pH 9.1 are shown in Figure 3.

The reaction at pH 7.4 did not result in a significant slowing of reaction rate relative to the reaction at pH 9.1, as determined by RP-HPLC monitoring of starting material peak height. In both cases, most of the starting reagent had reacted in the first few minutes. However, the reaction at pH 7.4 never provided a high yield of dityrosine-containing dimer (diATEE) as this dimer appeared to rapidly polymerise further before a significant yield could build-up. The reaction at pH 9.1, however, resulted in a rapid build-up of diATEE in the first two minutes, after which this product further reacted forming larger polymers (Figure 3). This time-course study clearly shows that diATEE can be formed in good yield if the reaction is not left too long. The optimum ratio of ATEE to HRP was found to be about 1:220.

To purify diATEE from the reaction mixture, the sample was desalted using flash C18 chromatography

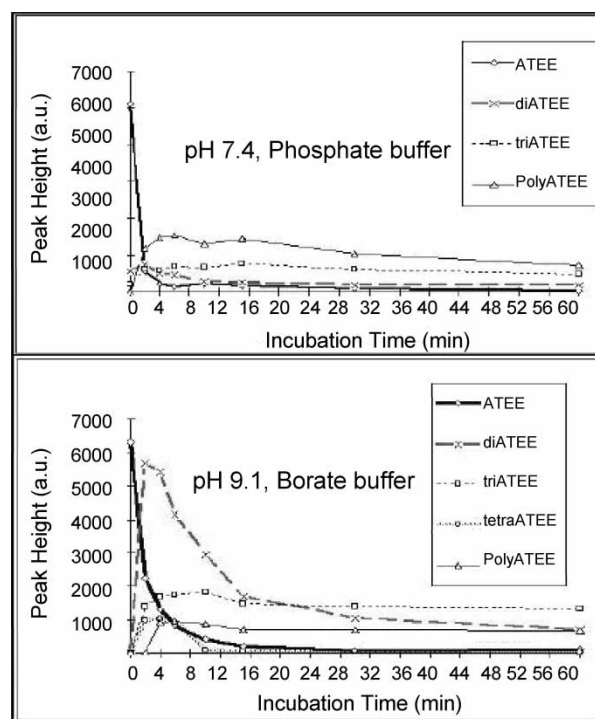


Figure 3. Time course study of dimerisation of ATEE using HRP at pH 7.4 and 9.1. Data are from the peak height at  $\lambda$ 280 nm from HPLC.

and then applied to RP-HPLC. The aqueous RP-HPLC phase required a lower level of TFA (0.01%) than that normally used for peptides, to avoid hydrolysis of the C-terminal ester bond. <sup>1</sup>H NMR resonances from the aromatic region (6.8–7.4 ppm) of the purified diATEE product are consistent with formation of a new carbon–carbon bond at the ortho positions of both tyrosine residues. Assignments are shown in Figure 4. The <sup>1</sup>H NMR values are in agreement with those previously reported for dityrosine [21] and theoretical values calculated using the ACD-HNMR (Toronto, Canada) integrated software package with a confidence of 95%.

### Dimerisation of A $\beta$ (9–16)

Dimerisation of A $\beta$ (9–16) was achieved under similar conditions to those used for ATEE. The reaction was monitored using a combination of RP-HPLC and ESI-MS. The reaction appeared to occur slower than for ATEE. Monitoring by RP-HPLC indicated that dimer formation reached a maximum at approximately 15 min, after which other polymeric reaction products slowly appear and the dimer yield decreases. It is not clear why the peptide reaction is significantly slower than that of ATEE under the same conditions, but it may be related to increased steric hindrance in the peptide due to the presence of other bulky amino acids.

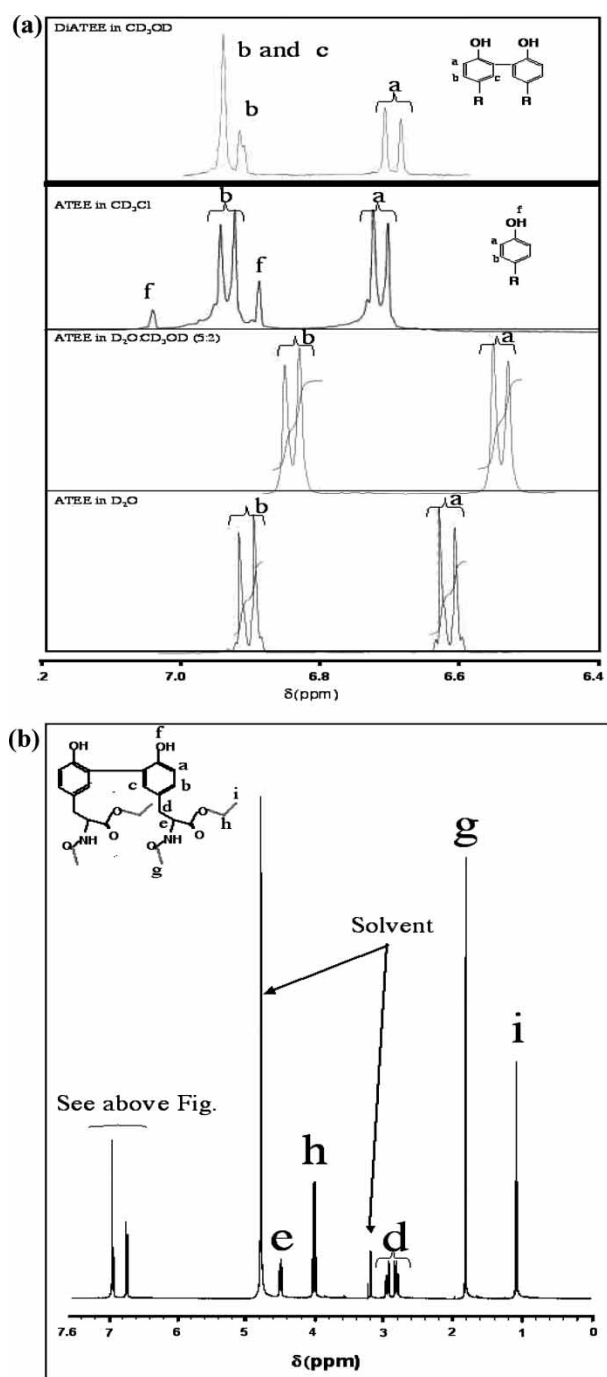


Figure 4. (a) Aromatic region of 400 MHz  $^1\text{H}$  NMR spectra of diATEE and ATEE in different solvents and (b) 400 MHz  $^1\text{H}$  NMR spectrum of diATEE in  $\text{CD}_3\text{OD}$ .

The slower reaction time of  $\text{A}\beta(9-16)$  relative to ATEE makes the peptide reaction more controllable and leads to an overall higher yield. Although, the yield after RP-HPLC purification was 22% by weight from tyrosine starting material, this yield is low due to losses during chromatography. The actual yield before purification was estimated by HPLC to be  $61 (\pm 6)\%$ . This yield was obtained by creating standard concentration vs peak area curves at 220 nm for both  $\text{A}\beta(9-16)$  and dimeric  $\text{A}\beta(9-16)$ , using purified

samples of both. Since the HPLC peaks were narrow, similar results were obtained either by peak height or area. The standard curves were then applied to quantitate both  $\text{A}\beta(9-16)$  and dimeric  $\text{A}\beta(9-16)$  in optimised reaction mixtures, to enable accurate quantitation of both compounds by RP-HPLC.

ESI-MS of the purified dimeric  $\text{A}\beta(9-16)$  product confirmed the presence of a dimer. A parent ion was observed at 1993.2 Da, consistent with the expected molecular weight of 1992.8 Da for  $[M + H]^+$ . Multiple charged species including  $2^+$  (997.1 Da),  $3^+$  (665.1 Da),  $4^+$  (499.1 Da) and  $5^+$  (399.4 Da) were also observed in the ESI-MS, confirming that the dimer observed was not one that was formed in the mass spectrometer. The UV and fluorescence spectrum of the product was also consistent with that observed for the dityrosine species observed for ATEE, supporting the formation of an ortho-ortho linkage between the two peptide tyrosines. For example, for both diATEE and dimeric  $\text{A}\beta(9-16)$ , the new UV maxima appeared at 251 and 294 nm. Observed  $\lambda_{\text{em}}$ , max at 274 and 325 nm were similar for both diATEE and dimeric  $\text{A}\beta(9-16)$  and consistent with that observed by Heinecke et al. for dityrosine [20]. Amino acid analysis of the purified dimer confirmed that all amino acids other than tyrosine were intact. No tyrosine was detected, also supporting that this residue had dimerised.

#### Dimerisation of $\text{A}\beta(1-28)$ and $\text{A}\beta(1-40)$

Reactions of  $\text{A}\beta(1-40)$  and  $\text{A}\beta(1-28)$  were carried out as above using the HRP/ $\text{H}_2\text{O}_2$  system. A fluorescence plate reader with two specific filters for tyrosine oxidation ( $\lambda_{\text{ex}}$  355 nm/ $\lambda_{\text{em}}$  460 nm, and  $\lambda_{\text{ex}}$  485 nm/ $\lambda_{\text{em}}$  538 nm [40]) was used to monitor the formation of dityrosine oligomers. These filters were used to monitor dityrosine formation as other oligomeric products have higher  $\lambda_{\text{ex}}$  and  $\lambda_{\text{em}}$ , and using  $\lambda_{\text{ex}}$  325/ $\lambda_{\text{em}}$  407 nm, normally used for tyrosine, is not recommended due to interference from His and Phe oxidation products [40]. The plate reader results showed formation of dityrosine-like products (Figure 5), as indicated from the elevation in fluorescence with both filters. Results were similar to those obtained for the ATEE control. The formation of  $\text{A}\beta(1-40)$  dimers has also been confirmed by Yoburn et al. [5,6] using similar reaction methods but much higher concentrations of reactants.

The HRP/ $\text{H}_2\text{O}_2$  reaction with  $\text{A}\beta(1-28)$  and  $\text{A}\beta(1-40)$  was also monitored using SDS-PAGE and antibody detection (WO2). The Gel/WO2 results (Figure 6) showed the formation of higher oligomer and indicate that the dimerisation promotes further aggregation into larger oligomers. Several attempts were made to ensure that the gel was not over-loaded but the peptides appeared to grossly oligomerize resulting in an almost continuous band and, in fact,

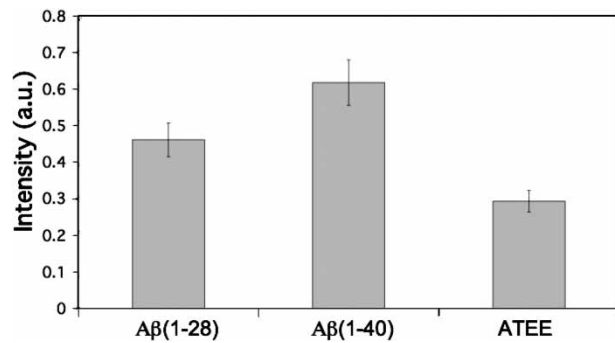


Figure 5. Results of HRP reaction with A $\beta$ (1-28), A $\beta$ (1-40) and ATEE monitored using a fluorescence plate reader ( $\lambda_{\text{ex}}485\text{ nm}/\lambda_{\text{em}}538\text{ nm}$ ). The results from three replicates are shown with error bars. (a.u. is arbitrary units).

the WO2 antibody appeared to be more sensitive to dityrosine formation in A $\beta$ (1-40) than the other A $\beta$  peptides. It is not known whether these larger oligomers are the result of covalent polymerisation or non-covalently linked peptide aggregates where aggregation is promoted by the initial formation of a covalent dityrosine dimer. Further work is needed to determine the biological significance of this increased aggregation. The gel results show that A $\beta$  modified by formation of dityrosine still binds WO2 antibodies. This demonstrates that dityrosine formation between A $\beta$  molecules has no effect on the detection of A $\beta$  by WO2 (epitope of WO2 is A $\beta$ (5-8)).

Our results show that ATEE can be used as a model for dityrosine formation in peptides. NMR analysis of the reaction product from ATEE indicates that the major dimer results from a new carbon-carbon bond linking the ortho positions of two tyrosine residues. This dityrosine formation is not reversible and results in the formation of a new amino acid (dityrosine) that

is fluorescent. We also have shown that A $\beta$  fragment dimers can be synthesised in relatively high yield using a procedure similar to Yoburn et al. [5,6], who recently published a method to dimerise A $\beta$ (8-14) and A $\beta$ (1-40). In addition, we demonstrate that A $\beta$  peptides, including A $\beta$ (1-40), can be dimerised and the time course of the reaction monitored by fluorescence spectroscopy and with a fluorescent plate reader. Gel electrophoresis indicated that formation of A $\beta$ (1-28) and A $\beta$ (1-40) dimers resulted in increased aggregation for these peptides. These dimeric A $\beta$  peptides may be useful for studying both the importance of early dimerisation in amyloid formation and the role of dityrosine formation in A $\beta$  neurotoxicity.

The neurotoxicity of these dimeric peptides remains to be determined. Tyr-10 is known to be important in amyloid formation and neurotoxicity, and a tyrosine to phenylalanine substitution is one of the three residue differences between the human and mouse A $\beta$  sequence. Non-transgenic mice do not form amyloid plaque and this is believed to be due to differences in their A $\beta$  sequence relative to humans, including the tyrosine to phenylalanine substitution. The formation of dityrosine-linkages is known to occur in a number of peptides and proteins [38,41], and is associated with aging [42-44]. Dityrosine-linkage may play a role in forming higher oligomers of A $\beta$  and may be important in the pathogenesis associated with AD. MPO has been reported to be present in human AD plaques [45] and further study is necessary to determine if MPO could induce dityrosine formation under more physiological conditions. The results presented here provide methods for the synthesis and monitoring of dityrosine-containing peptides and, in particular, A $\beta$  peptides. These methods may be useful

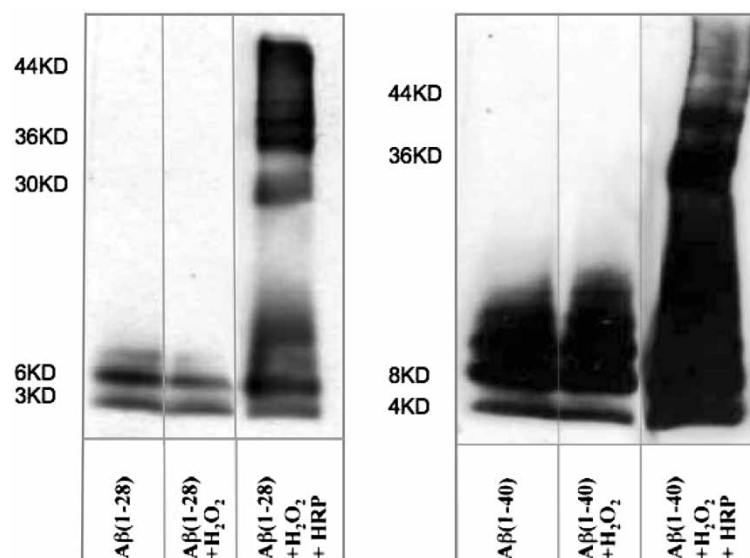


Figure 6. Gel/WO2 electrophoresis results of A $\beta$  HRP/H<sub>2</sub>O<sub>2</sub> reaction, showing the formation of multiple oligomers of A $\beta$ .

for investigating the role of A $\beta$  metal binding, oxidative damage and dityrosine formation in amyloid formation and neurodegeneration in AD.

## Conclusions

In this study, we report chromatographic and spectroscopic techniques for the preparation, isolation and analysis of dityrosine as either a protected amino acid or as part of a peptide. Optimum conditions for dimerisation of ATEE and A $\beta$ (9–16) peptide dimers using HRP are described. The method does not require protection and deprotection of functional groups and demonstrates the utility of peroxidases for formation of *o,o'*-dityrosine. Dimeric A $\beta$ (9–16) was obtained in reasonable yield and purity, without modification of other residues, notably histidine and phenylalanine (Figure 7).

Our results also demonstrate that dityrosine-linkage can lead to oligomerisation of A $\beta$  peptides. Dityrosine modification could be an early pathological event in A $\beta$  deposition in AD. A recent study has shown that the substitution of tyrosine with alanine in the A $\beta$  sequence inhibits the ability of this peptide to catalyse the production of H<sub>2</sub>O<sub>2</sub> and to cross-link, as well as inhibiting A $\beta$  neurotoxicity [8]. The role of dityrosine-linkages in the aggregation and neurotoxicity of A $\beta$  needs further investigation both *in vitro* and *in vivo*. The application of the methods described here for the formation and monitoring of A $\beta$  dityrosine formation

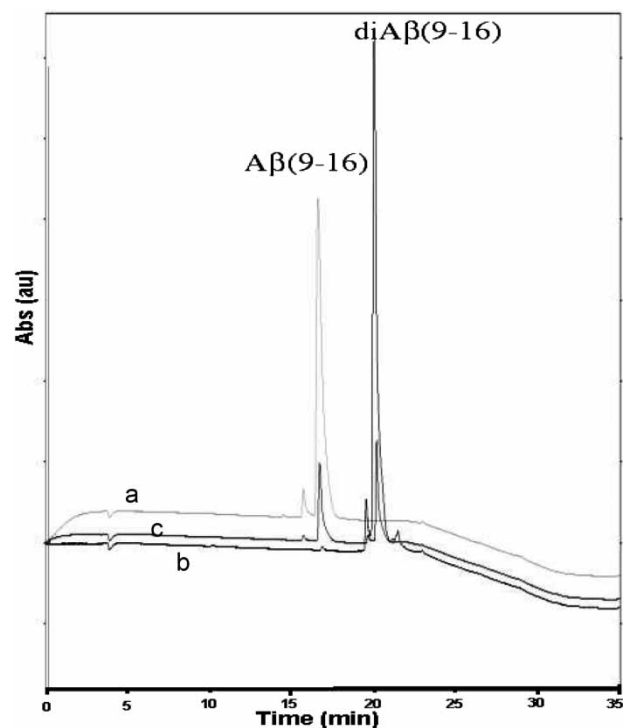


Figure 7. The chromatograms of A $\beta$ (9–16) and A $\beta$ (9–16) dimer (diA $\beta$ (9–16)) standards; (a) 1 mg/ml of A $\beta$ (9–16), (b) diA $\beta$ (9–16) and (c) mixture of 0.2 mg/ml of both A $\beta$ (9–16) and diA $\beta$ (9–16).

should be useful for exploring the role of A $\beta$  dimerisation and dityrosine formation in amyloid formation and neurodegeneration in AD.

## Acknowledgements

F.E.A. would like to thank University of Melbourne for MIRS, APA and Loxton Bequest Scholarships. In addition, we would like to thank MRDGS and ARC for financial support.

## References

- [1] Butterfield DA, Lauderback CM. Lipid peroxidation and protein oxidation in Alzheimer's disease brain: Potential causes and consequences involving amyloid beta-peptide-associated free radical oxidative stress [Review]. *Free Radic Biol Med* 2002;32(11):1050–1060.
- [2] Dong J, Atwood CS, Anderson VE, Siedlak SL, Smith MA, Perry G, Carey PR. Metal binding and oxidation of amyloid-beta within isolated senile plaque cores: Raman microscopic evidence. *Biochemistry* 2003;42(10):2768–2773.
- [3] Yang C. An *i*-4, *i*, *i*+4 reductive and nucleophilic zipper shared by both prion protein and beta-amyloid peptide sequences supports a common putative molecular mechanism. *Chem J Internet* 2000;2(7):35, [www.chemistrymag.org/cji/2000/027035le.htm](http://www.chemistrymag.org/cji/2000/027035le.htm).
- [4] Ali FE, Barnham KJ, Barrow CJ, Separovic F. Metal catalyzed oxidative damage and oligomerization of the amyloid- $\beta$  peptide (A $\beta$ ) of Alzheimer's disease. *Aust J Chem* 2004;57:507–518.
- [5] Ali FE, Barnham KJ, Barrow CJ, Separovic F. Copper catalysed oxidation of amino acids and Alzheimer's disease. *Lett Pept Sci* 2004;10(5-6):405–412.
- [6] Yoburn JC, Tian W, Brower JO, Nowick JS, Glabe CG, Van Vranken DL. Dityrosine cross-linked A $\beta$  peptides: Fibrillar  $\beta$ -structure in A $\beta$ (1–40) is conducive to formation of dityrosine cross-links but a dityrosine cross-link in A $\beta$ (8–14) does not induce  $\beta$ -structure. *Chem Res Toxicol* 2003;16(4):531–535.
- [7] Fancy DA, Kodadek T. A critical role for tyrosine residues in His(6)Ni-mediated protein cross-linking. *Biochem Biophys Res Commun* 1998;247(2):420–426.
- [8] Barnham KJ, Haeffner F, Ciccotosto GD, Curtain CC, Tew D, Mavros C, Beyreuther K, Carrington D, Masters CL, Cherny RA, Cappai R, Bush AI. Tyrosine gated electron transfer is key to the toxicity mechanism of Alzheimer's disease  $\beta$ -amyloid. *FASEB J* 2004;18(12):1427–1429.
- [9] Atwood CS, Perry G, Zeng H, Kato Y, Jones WD, Ling K-Q, Huang X, Moir RD, Wang D, Sayre LM, Smith MA, Chen SG, Bush AI. Copper mediates dityrosine cross-linking of Alzheimer's amyloid- $\beta$ . *Biochemistry* 2004;43(2):560–568.
- [10] Eickhoff H, Jung G, Rieker A. Oxidative phenol coupling—tyrosine dimers and libraries containing tyrosyl peptide dimers. *Tetrahedron* 2001;57(2):353–364.
- [11] Shamovsky IL, Riopelle RJ, Ross GM. *Ab initio* studies on the mechanism of tyrosine coupling. *J Phys Chem A* 2001;105(6):1061–1070.
- [12] Baudry N, Lejeune PJ, Niccoli P, Vinet L, Carayon P, Mallet B. Dityrosine bridge formation and thyroid hormone synthesis are tightly linked and are both dependent on N-glycans. *FEBS Lett* 1996;396(2-3):223–226.
- [13] Kanwar R, Balasubramanian D. Structural studies on some dityrosine-cross-linked globular proteins: Stability is weakened, but activity is not abolished. *Biochemistry* 2000;39(48):14976–14983.



- [14] Malencik DA, Anderson SR. Dityrosine formation in calmodulin. *Biochemistry* 1987;26(3):695–704.
- [15] Malencik DA, Anderson SR. Dityrosine formation in calmodulin—cross-linking and polymerization catalyzed by arthromyces peroxidase. *Biochemistry* 1996;35(14):4375–4386.
- [16] Guerin MC, Torreilles J. Lipid peroxidation by peroxidase-catalyzed bioactivation of tyrosine. *Redox Rep* 1995;1(4):287–290.
- [17] Heinecke JW. Mechanisms of oxidative damage by myeloperoxidase in atherosclerosis and other inflammatory disorders. *J Lab Clin Med* 1999;133(4):321–325.
- [18] Francis GA, Mendez AJ, Bierman EL, Heinecke JW. Oxidative tyrosylation of high density lipoprotein by peroxidase enhances cholesterol removal from cultured fibroblasts and macrophage foam cells. *Proc Natl Acad Sci USA* 1993;90(14):6631–6635.
- [19] Heinecke JW, Li W, Francis GA, Goldstein JA. Tyrosyl radical generated by myeloperoxidase catalyzes the oxidative cross-linking of proteins. *J Clin Investing* 1993;91(6):2866–2872.
- [20] Heinecke JW, Li W, Daehnke III, HL, Goldstein JA. Dityrosine, a specific marker of oxidation, is synthesized by the myeloperoxidase-hydrogen peroxide system of human neutrophils and macrophages. *J Biol Chem* 1993;268(6):4069–4077.
- [21] Jacob JS, Cistola DP, Hsu FF, Muzaffar S, Mueller DM, Hazen SL, Heinecke JW. Human phagocytes employ the myeloperoxidase-hydrogen peroxide system to synthesize dityrosine, trityrosine, pulcherosine, and isodityrosine by a tyrosyl radical-dependent pathway. *J Biol Chem* 1996;271(33):19950–19956.
- [22] Marquez LA, Dunford HB. Kinetics of oxidation of tyrosine and dityrosine by myeloperoxidase compounds i and ii—implications for lipoprotein peroxidation studies. *J Biol Chem* 1995;270(51):30434–30440.
- [23] Savenkova MI, Mueller DM, Heinecke JW. Tyrosyl radical generated by myeloperoxidase is a physiological catalyst for the initiation of lipid peroxidation in low density lipoprotein. *J Biol Chem* 1994;269(32):20394–20400.
- [24] Stanbro WD. A kinetic model of the myeloperoxidase hydrogen peroxide chloride ion system in phagolysosomes. *J Theor Biol* 1998;193(1):59–68.
- [25] Winterbourn CC, Pichorner H, Kettle AJ. Myeloperoxidase-dependent generation of a tyrosine peroxide by neutrophils. *Arch Biochem Biophys* 1997;338(1):15–21.
- [26] Salmantabcheh S, Rabgaoui N, Torreilles J. Neutrophil-catalysed dimerisation of tyrosyl peptides. *Free Radic Res Commun* 1993;19(4):217–227.
- [27] Foppoli C, Demarco C, Blarmino C, Coccia R, Mosca L, Rosei MA. Dimer formation by cytochrome c-catalyzed oxidation of tyrosine and enkephalins. *Amino Acids* 1997;13(3-4):273–280.
- [28] Leeuwenburgh C, Hansen PA, Holloszy JO, Heinecke JW. Hydroxyl radical generation during exercise increases mitochondrial protein oxidation and levels of urinary dityrosine. *Free Radic Biol Med* 1999;27(1-2):186–192.
- [29] Hensley K, Mait ML, Yu Z, Sang H, Markesbery WR, Floyd RA. Electrochemical analysis of protein nitrotyrosine and dityrosine in the Alzheimer brain indicates region-specific accumulation. *J Neurol Sci* 1998;18(20):8126–8132.
- [30] Onorato JM, Thorpe SR, Baynes JW. Immunohistochemical and ELISA assays for biomarkers of oxidative stress in aging and disease. *Ann N Y Acad Sci* 1998;854:277–290, Towards Prolongation of the Health Life Span.
- [31] Galeazzi L, Ronchi P, Franceschi C, Giunta S. *In vitro* peroxidase oxidation induces stable dimers of  $\beta$ -amyloid (1–42) through dityrosine bridge formation. *Amyloid* 1999;6(1):7–13.
- [32] Kadlcik V, Sicard-Roselli C, Mattioli TA, Kodicek M, Houee-Levin C. One-electron oxidation of  $\beta$ -amyloid peptide: Sequence modulation of reactivity. *Free Radic Biol Med* 2004;37(6):881–891.
- [33] Walsh DM, Tseng BP, Rydel RE, Podlisny MB, Selkoe DJ. The oligomerization of amyloid  $\beta$ -protein begins intracellularly in cells derived from human brain. *Biochemistry* 2000;39(35):10831–10839.
- [34] Guo ZW, Machiya K, Salamonczyk GM, Sih CJ. Total synthesis of bastadins 2, 3, and 6. *J Org Chem* 1998;63(13):4269–4276.
- [35] He W, Barrow CJ. The A $\beta$  3-pyroglutamy and 11-pyroglutamy peptides found in senile plaque have greater  $\beta$ -sheet forming and aggregation propensities *in vitro* than full-length A $\beta$ . *Biochemistry* 1999;38(33):10871–10877.
- [36] Cherny RA, Legg JT, McLean CA, Fairlie DP, Huang X, Atwood CS, Beyreuther K, Tanzi RE, Masters CL, Bush AI. Aqueous dissolution of Alzheimer's disease A $\beta$  amyloid deposits by biometal depletion. *J Biol Chem* 1999;274(33):23223–23228.
- [37] Ida N, Hartmann T, Pantel J, Schroder J, Zerfass R, Forstl H, Sandbrink R, Masters CL, Beyreuther K. Analysis of heterogeneous A4 peptides in human cerebrospinal fluid and blood by a newly developed sensitive Western blot assay. *J Biol Chem* 1996;271(37):22908–22914.
- [38] Kato Y, Kitamoto N, Kawai Y, Osawa T. The hydrogen peroxide/copper ion system, but not other metal-catalyzed oxidation systems, produces protein-bound dityrosine. *Free Radic Biol Med* 2001;31(5):624–632.
- [39] Malanik V, Ledvina M. Preparation and isolation of dityrosine. *Prep Biochem* 1979;9(3):273–280.
- [40] Ali FE, Separovic F, Barrow CJ, Cherny RA, Fraser F, Bush AI, Masters CL, Barnham KJ. Methionine regulates copper/hydrogen peroxide oxidation products of A $\beta$ . *J Pept Sci* 2005;11:353–360.
- [41] Huggins TG, Wells-Knecht MC, Detorie NA, Baynes JW, Thorpe SR. Formation of o-tyrosine and dityrosine in proteins during radiolytic and metal-catalyzed oxidation. *J Biol Chem* 1993;268(17):12341–12347.
- [42] Kato Y, Maruyama W, Naoi M, Hashizume Y, Osawa T. Immunohistochemical detection of dityrosine in lipofuscin pigments in the aged human brain. *FEBS Lett* 1998;439(3):231–234.
- [43] Wells-Knecht MC, Huggins TG, Dyer DG, Thorpe SR, Baynes JW. Oxidized amino acids in lens protein with age—measurement of o-tyrosine and dityrosine in the aging human lens. *J Biol Chem* 1993;268(17):12348–12352.
- [44] Leeuwenburgh C, Wagner P, Holloszy JO, Sohal RS, Heinecke JW. Caloric restriction attenuates dityrosine cross-linking of cardiac and skeletal muscle proteins in aging mice. *Arch Biochem Biophys* 1997;346(1):74–80.
- [45] Green PS, Mendez AJ, Jacob JS, Crowley JR, Growdon W, Hyman BT, Heinecke JW. Neuronal expression of myeloperoxidase is increased in Alzheimer's disease. *J Neurochem* 2004;90:724–733.